

Excitation of atoms in an optical lattice driven by polychromatic amplitude modulation

Linxiao Niu, Dong Hu, Shengjie Jin, Xiangyu Dong, Xuzong Chen, and
Xiaoji Zhou*

*School of Electronics Engineering & Computer Science, Peking University, Beijing 100871,
China*

[*xjzhou@pku.edu.cn](mailto:xjzhou@pku.edu.cn)

Abstract: We investigate the multiphoton process between different Bloch states in an amplitude modulated optical lattice. In the experiment, we perform the modulation with more than one frequency components, which includes a high degree of freedom and provides a flexible way to coherently control quantum states. Based on the study of single frequency modulation, we investigate the collaborative effect of different frequency components in two aspects. Through double frequency modulations, the spectrums of excitation rates for different lattice depths are measured. Moreover, interference between two separated excitation paths is shown, emphasizing the influence of modulation phases when two modulation frequencies are commensurate. Finally, we demonstrate the application of the double frequency modulation to design a large-momentum-transfer beam splitter. The beam splitter is easy in practice and would not introduce phase shift between two arms.

© 2021 Optical Society of America

OCIS codes: (020.1475) Bose-Einstein condensates; (020.1670) Coherent optical effects; (270.0270) Quantum optics.

References and links

1. J. Struck, C. Ölschläger, M. Weinberg, P. Hauke, J. Simonet, A. Eckardt, M. Lewenstein, K. Sengstock, and P. Windpassinger, "Tunable gauge potential for neutral and spinless particles in driven optical lattices," *Phys. Rev. Lett.* **108**, 225304 (2012).
2. P. Hauke, O. Tieleman, A. Celi, C. Ölschläger, J. Simonet, J. Struck, M. Weinberg, P. Windpassinger, K. Sengstock, M. Lewenstein, and A. Eckardt, "Non-Abelian gauge fields and topological insulators in shaken optical lattices," *Phys. Rev. Lett.* **109**, 145301 (2012).
3. J. Struck, M. Weinberg, C. Ölschläger, P. Windpassinger, J. Simonet, K. Sengstock, R. Höppner, P. Hauke, A. Eckardt, M. Lewenstein, and L. Mathey, "Engineering Ising-XY spin-models in a triangular lattice using tunable artificial gauge fields," *Nature Phys.* **9**, 738–743 (2013).
4. A. Alberti, V. V. Ivanov, G. M. Tino, and G. Ferrari, "Engineering the quantum transport of atomic wavefunctions over macroscopic distances," *Nature Phys.* **5**, 547–550 (2009).
5. A. Zenesini, H. Lignier, D. Ciampini, O. Morsch, and E. Arimondo, "Coherent control of dressed matter waves," *Phys. Rev. Lett.* **102**, 100403 (2009).
6. K. Hai, Y. Luo, G. Lu, and W. Hai, "Phase-controlled localization and directed transport in an optical bipartite lattice," *Opt. Express* **22**, 4277–4289 (2014).
7. C. V. Parker, L. C. Ha and C. Chin, "Direct observation of effective ferromagnetic domains of cold atoms in a shaken optical lattice," *Nat. Phys.* **9**, 769–774 (2013).
8. J. H. Denschlag, J. E. Simsarian, H. Häffner, C. McKenzie, A. Browaeys, D. Cho, K. Helmerson, S. L. Rolston and W. D. Phillips, "A Bose-Einstein condensate in an optical lattice," *J. Phys. B* **35**, 3095–3110 (2002).

9. T. Stöferle, H. Moritz, C. Schori, M. Köhl, and T. Esslinger, “Transition from a strongly interacting 1D superfluid to a Mott insulator,” *Phys. Rev. Lett.* **92**, 130403 (2004).
10. W. K. Hensinger, H. Häffner, A. Browaeys, N. R. Heckenberg, K. Helmerson, C. McKenzie, G. J. Milburn, W. D. Phillips, S. L. Rolston, H. Rubinsztein-Dunlop, and B. Upcroft, “Dynamical tunnelling of ultracold atoms,” *Nature* **412**, 52–55 (2001).
11. D. A. Steck, W. H. Oskay, M. G. Raizen, “Observation of chaos-assisted tunneling between islands of stability,” *Science* **293**, 274–278 (2001).
12. P. Cheiney, C. M. Fabre, F. Vermersch, G. L. Gattobigio, R. Mathevet, T. Lahaye, and D. Guéry-Odelin, “Matter-wave scattering on an amplitude-modulated optical lattice,” *Phys. Rev. A* **87**, 013623 (2013).
13. A. Alberti, G. Ferrari, V. V. Ivanov, M. L. Chiofalo, and G. M. Tino, “Atomic wave packets in amplitude-modulated vertical optical lattices,” *New J. Phys.* **12**, 065037 (2010).
14. N. Poli, F.-Y. Wang, M. G. Tarallo, A. Alberti, M. Prevedelli, and G. M. Tino, “Precision measurement of gravity with cold atoms in an optical lattice and comparison with a classical gravimeter,” *Phys. Rev. Lett.* **106**, 038501 (2011).
15. P. Cladé, S. Guellati-Khélifa, F. Nez, and F. Biraben, “Large momentum beam splitter using Bloch oscillations,” *Phys. Rev. Lett.* **102**, 240402 (2009).
16. M. Kozuma, L. Deng, E. W. Hagley, J. Wen, R. Lutwak, K. Helmerson, S. L. Rolston, and W. D. Phillips, “Coherent splitting of Bose-Einstein condensed atoms with optically induced Bragg diffraction,” *Phys. Rev. Lett.* **82**, 871–875 (1999).
17. A. Gómez-León and G. Platero, “Floquet-Bloch theory and topology in periodically driven lattices,” *Phys. Rev. Lett.* **110**, 200403 (2013).
18. S.-I. Chu and D. A. Telnov, “Beyond the Floquet theorem: generalized Floquet formalisms and quasienergy methods for atomic and molecular multiphoton processes in intense laser fields,” *Phys. Rep.* **390**, 1–131 (2004).
19. O. Morsch, J. H. Müller, M. Cristiani, D. Ciampini, and E. Arimondo, “Bloch oscillations and mean-field effects of Bose-Einstein condensates in 1D optical lattices,” *Phys. Rev. Lett.* **87**, 140402 (2001).
20. D. Choi and Q. Niu, “Bose-Einstein condensates in an optical lattice,” *Phys. Rev. Lett.* **82**, 2022 (1999).
21. X. X. Liu, X. J. Zhou, W. Xiong, T. Vogt, and X. Z. Chen, “Rapid nonadiabatic loading in an optical lattice,” *Phys. Rev. A* **83**, 063402 (2011).
22. Y. Y. Zhai, X. G. Yue, Y. J. Wu, X. Z. Chen, P. Zhang, and X. J. Zhou, “Effective preparation and collisional decay of atomic condensates in excited bands of an optical lattice,” *Phys. Rev. A* **87**, 063638 (2013).
23. T. Salger, S. Kling, S. Denisov, A. V. Ponomarev, P. Hänggi, and M. Weitz, “Tuning the mobility of a driven Bose-Einstein condensate via diabatic Floquet bands,” *Phys. Rev. Lett.* **110**, 135302 (2013).
24. D. Döring, J. E. Debs, N. P. Robins, C. Figl, P. A. Altin, and J. D. Close, “Ramsey interferometry with an atom laser,” *Opt. Express* **17**, 20661–20668 (2009).
25. W. Zheng and H. Zhai, “Floquet topological states in shaking optical lattices,” *Phys. Rev. A* **89**, 061603 (2014).
26. S.-L. Zhang and Q. Zhou, “Shaping topological properties of the band structures in a shaken optical lattice,” *Phys. Rev. A* **90**, 051601 (2014).

1. Introduction

Ultracold atoms in periodically driven optical lattices, including shaken and amplitude modulated systems, have attracted much attention recent years, for they can bring out new interesting phenomena including realization of artificial gauge fields in different lattice geometries [1–3] and the coherent control of atomic wavefunctions [4–6]. In a shaken one dimensional optical lattice, the ferromagnetic transition in trapped Bose gas has also been observed [7] by coupling ground band s of the lattice system to the first excited band p . Specific to amplitude modulated lattice systems, although only bands with the same parity can be coupled, there are still researches on a wide range of problems, such as transfer of atoms from the ground band s to the second excited band d [8], detection of superfluid-Mott insulator transition [9] and study of the dynamical tunnelling of ultracold atoms with quantum chaos [10, 11]. The technique can also be applied in areas including realization of a velocity filter [12] and detection of gravity [13, 14].

Normally, studies of amplitude modulated lattices are based on single frequency modulations that only involve processes with one photon emission or absorption. During a polychromatic modulation, not only the amplitudes, but also the phases of different frequency components in the modulation can be controlled independently, providing a more flexible way to coherently manipulate quantum states. In this paper, we coherently transfer atoms from the ground state s to the high excited g band via a double frequency modulation. The peaks of transfer rate with

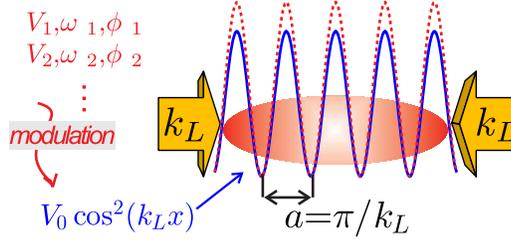


Fig. 1. A sketch of lattice depth modulation in our system. The depth of lattice potential $V_0 \cos^2(k_L x)$ is driven by a polychromatic modulation $\sum_i V_i \cos(\omega_i t + \phi_i)$.

different lattice depths are measured experimentally, while influence of the modulation phase is demonstrated by performing an interference between two independent paths of excitations. These experiments completely investigated how frequencies and phases of different modulation frequency components would influence the excitation between Bloch states. Furthermore, we show an application of the double frequency modulation to build a large-momentum-transfer (LMT) beam splitter. Comparing with LMT beam splitters based on Bloch oscillation [8, 15] or high order Bragg scattering [16], our method is easy in practise and would not introduce phase shift between two separated atom clouds.

The paper is organized as follows: In Sections 2 and 3 the polychromatic modulation theory based on Floquet method and our experimental system are introduced respectively. In Section 4, we study the effects of the modulation phase for the single frequency modulation. In Section 5 collaborative effect of different frequency components is studied, demonstrate the effect of both modulation frequencies and phases. Section 6 presents a way to realize a LMT beam splitter. Discussion and conclusion are in Section 7.

2. Theory for optical lattice with polychromatic modulation

For an atom in an amplitude modulated lattice system along \hat{x} axis, as schematically shown in Fig. 1, the time dependent Hamiltonian can be written as

$$H(t) = \frac{p_x^2}{2M} + V_0 \cos^2(k_L x) + \sum_i V_i \cos(\omega_i t + \phi_i) \cos^2(k_L x). \quad (1)$$

The first term in the right hand side is kinetic energy with M the atom's mass and p_x its momentum along the x direction. The second term represents optical lattice without the modulation. V_0 is the constant part of the lattice depth, and the wave vector is $k_L = 2\pi/\lambda$ with λ the laser wavelength. The last term expresses the amplitude modulation with the modulation amplitude V_i , the frequency ω_i and the phase ϕ_i of each frequency components.

Typically, time-periodic systems are described by Floquet's theorem [17]. In our system, each of the modulation frequencies ω_i gives a period $T_i = 2\pi/\omega_i$ and the Hamiltonian has a period of $H(t+T) = H(t)$, with T the lowest common multiple of T_i . By defining a time-evolution operator for one period as $\hat{U}(T)$, solutions to this problem must satisfy

$$|\psi_{q,\alpha}(t+T)\rangle = \hat{U}(T)|\psi_{q,\alpha}(t)\rangle = e^{i\varepsilon_{q,\alpha}T}|\psi_{q,\alpha}(t)\rangle, \quad (2)$$

and the Floquet states $|u_{q,\alpha}\rangle$ are defined as $|\psi_{q,\alpha}\rangle = e^{iqx - i\varepsilon_{q,\alpha}t}|u_{q,\alpha}\rangle$ with the quasi-momentum q , the band index α and quasi-energy $\varepsilon_{q,\alpha}$, which leads to

$$(H(t) - i\partial_t)|u_{q,\alpha}\rangle = H_0|u_{q,\alpha}\rangle = \varepsilon_{q,\alpha}|u_{q,\alpha}\rangle. \quad (3)$$

For a special case of single frequency modulation, considering the time and coordinate periodicity of the Floquet states $|u_{q,\alpha}\rangle$, by a Fourier transformation we can study the problem with a set of basis $|v_{lm}\rangle = e^{i(2lk_L x - m\omega_1 t)}$ in an extended Hilbert space $\mathcal{S} = \mathcal{H} \otimes \mathcal{T}$. Where \mathcal{H} is the Hilbert space and \mathcal{T} is the space of all functions with periodic T . By integration in one period, we can turn to a time-independent system.

$$A_{lm,l'm'} = \frac{1}{T} \int_0^T |v_{l'm'}\rangle H_0 \langle v_{lm}| dt. \quad (4)$$

To get rid of the phase ϕ_1 , we perform an unitary transformation $U_{lm,lm} = e^{im\phi_1}$ to the Hamiltonian by $A' = U^{-1}AU$. There are three kinds of terms in the matrix of A' . The diagonal terms $A'_{lm;lm} = (2l\hbar k_L)^2/2M + m\hbar\omega_1$ are the energy of momentum states shifted by absorbing or emitting Floquet photons with energy $\hbar\omega_1$. The terms $A'_{lm;l\pm 1,m} = V_0/4$ show stationary component of the lattice would coupling atoms with momentum difference $2\hbar k_L$. In addition, $A'_{lm;l\pm 1,m\pm 1} = V_1/8$ terms show the time modulation of the lattice, which would coupling two momentum states separated by $2\hbar k_L$ while absorbing or emitting one Floquet photon.

When the modulation frequency is near-resonant with the energy difference between two specific bands and far detuned from the others, we can get an effective Hamiltonian by a rotating wave approximation.

$$H_R = \begin{pmatrix} E_\alpha & V_1 e^{i\phi_1} \Omega_{\alpha\beta} \\ V_1 e^{-i\phi_1} \Omega_{\alpha\beta}^* & E_\beta - \hbar\omega \end{pmatrix}, \quad (5)$$

where E_α and E_β are the energy of Bloch states $|\alpha\rangle, |\beta\rangle$ in the system without modulation. Coupling constant between two states is $\Omega_{\alpha\beta} = \langle \alpha | \cos^2(k_L x) | \beta \rangle / 4$.

The extension to polychromatic driven is straightforward. For example, a double frequency modulation induced two-photon process between s - g band is described by an effective Hamiltonian H_{sg} as:

$$H_{sg} = \begin{pmatrix} E_s & e^{i\phi_1} V_1 \Omega_{sd} & e^{i\phi_2} V_2 \Omega_{sd} & 0 & 0 & 0 \\ e^{-i\phi_1} V_1 \Omega_{sd}^* & E_d - \hbar\omega_1 & 0 & e^{i\phi_2} V_2 \Omega_{dg} & e^{i\phi_1} V_1 \Omega_{dg} & 0 \\ e^{-i\phi_2} V_2 \Omega_{sd}^* & 0 & E_d - \hbar\omega_2 & e^{i\phi_1} V_1 \Omega_{dg} & 0 & e^{i\phi_2} V_2 \Omega_{dg} \\ 0 & e^{-i\phi_2} V_2 \Omega_{dg}^* & e^{-i\phi_1} V_1 \Omega_{dg}^* & E_g - \hbar(\omega_1 + \omega_2) & 0 & 0 \\ 0 & e^{-i\phi_1} V_1 \Omega_{dg}^* & 0 & 0 & E_g - 2\hbar\omega_1 & 0 \\ 0 & 0 & e^{-i\phi_2} V_2 \Omega_{dg}^* & 0 & 0 & E_g - 2\hbar\omega_2 \end{pmatrix}, \quad (6)$$

The effective Hamiltonian H_{sg} is constructed by means of nearly degenerate perturbation technique [18], in which we include six nearly degenerate states considering four main processes in the excitation. The six states are $|E_s\rangle$ the s band, $|E_d - \hbar\omega_1\rangle, |E_d - \hbar\omega_2\rangle$ the d band dressed by Floquet photon ω_1 or ω_2 and $|E_g - \hbar(\omega_1 + \omega_2)\rangle, |E_g - 2\hbar\omega_1\rangle$ and $|E_g - 2\hbar\omega_2\rangle$ the g band dressed by two Floquet photons. Using this basis a general state $(v_1, v_2, v_3, v_4, v_5, v_6)^T$ gives complex coefficient of the six dressed states. Population of Bloch states s is $|v_1|^2$, while population on g band is $|v_4 e^{i(\omega_1 + \omega_2)t} + v_5 e^{2i\omega_1 t} + v_6 e^{2i\omega_2 t}|^2$, given by coherent superposition of all g band states dressed with different Floquet photons. Solution of the model consists with the time dependent Schrödinger equation and the effective model provides us a better understanding of the multiphoton process. However, in the calculation more states associated with higher order processes could be included to get a more accurate result, especially when the modulation amplitude is large.

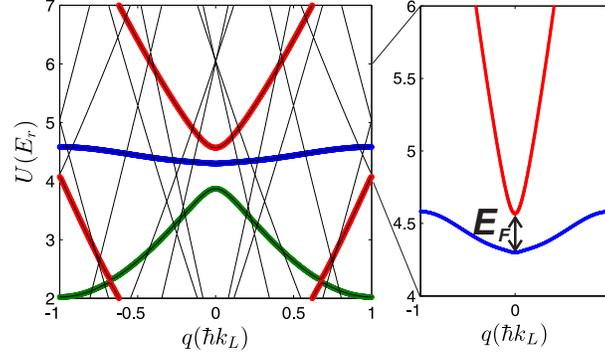


Fig. 2. Left side is the calculated Floquet spectra of a single frequency driven system, with parameters $V_0 = 5E_r$, $V_1 = 0.5E_r$, $\hbar\omega_1 = 5E_r$. In the figure the first seven bands are presented. The heavy lines depict states maximally overlapping with the s (blue), p (green) and d (red) Bloch bands respectively. Right side shows the details of two Floquet bands most overlapping with s and d bands. The two bands are separated by a band gap E_F at $q=0$.

3. Experimental system

Our experiment begins with a quasi-pure condensate of typically 1.5×10^5 ^{87}Rb atoms in the $|F = 2, m_F = 2\rangle$ hyperfine ground state, produced in a combined potential of a single-beam optical dipole trap and a quadrupole magnetic trap. The trapping frequencies are $\omega_x = 2\pi \times 28\text{Hz}$, $\omega_y = 2\pi \times 60\text{Hz}$, $\omega_z = 2\pi \times 70\text{Hz}$. The optical lattice is formed by a retro-reflected red detuned laser beam, with lattice constant $a = \lambda/2 = 426\text{nm}$ focused to a waist of $110\mu\text{m}$. Density of atoms in our system is less than $5 \times 10^{13}\text{cm}^{-3}$, and the mean-field interaction can be omitted to capture the main physical mechanism in the excitation [19, 20].

The lattice depth is calibrated by Kapitza-Dirac scattering and the modulation of lattice depth is controlled by an acousto-optic modulator (AOM). The modulation amplitudes V_i and phases ϕ_i are generated from a signal generator and the intensity of lattice laser is monitored by a photodetector. Experimental results are absorption images taken after 28ms time-of-flight (TOF). Occupation number at different momentum states $|2l\hbar k_L\rangle$ (l is integral momentum index) can be given from TOF images by $n_l = N_l/N$, with N_l the atom number at momentum state $|2l\hbar k_L\rangle$ and N the total atom number. The initial state for experiment is prepared non-adiabatically with numerically designed sequence of lattice pulses [21, 22]. For experimental convenience, the lattice pulses are carried out with the same depth as the constant part of the modulated lattice potential V_0 . Typically, each of the pulses and the subsequent intervals are lasting for no more than $25\mu\text{s}$, and the whole process can be finished within $60\mu\text{s}$, thus the loading time is greatly reduced comparing with traditional adiabatic loading method.

4. The initial phase effect in single frequency modulation

Single frequency modulation can be seen as the basis of polychromatic driven. In this part, we present the preparation of a Floquet state in the single frequency driven system, which is shown to be highly related to the modulation phase.

Following the discussion in Sec. 2, Fig. 2 depicts a typical quasi-energy spectrum of the single frequency driven system, which is obtained by direct diagonalization of A' at various quasi-momentum q . The same calculation also gives eigenvectors in the extended Hilbert space. The spectrum exhibits a complex structure as a result of the periodically repetition of high excited bands.

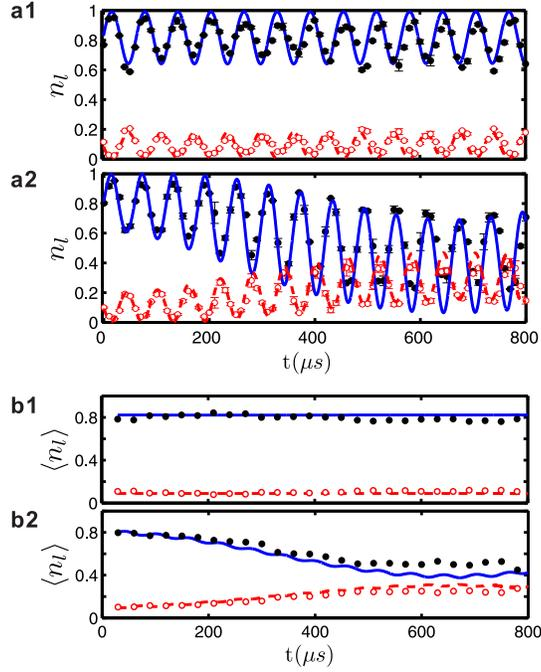


Fig. 3. Time evolution of n_l measured from the experiments with initial modulation phase (a1) $\phi = -\pi/2$ and (a2) $\phi = \pi/2$. Time averaged fraction $\langle n_l \rangle$ are also shown for (b1) $\phi = -\pi/2$ and (b2) $\phi = \pi/2$ respectively. n_0 is shown with black dots comparing to the numerical simulation in solid lines. n_1 and n_{-1} are shown in average with red circles the corresponding numerical result is shown in dashed lines. Each point is averaged by three experiments and the error bars indicate the standard deviation.

To connect our calculation with the experiments, we should project the Floquet states $|u_{q,\alpha}\rangle$ into momentum space. The occupation number at momentum states $|2l\hbar k_L\rangle$ and its phase can be given by a summation of all the Fourier components with the same l as $c_l(t)|2l\hbar k_L\rangle = \sum_m e^{-im\omega_1\tau} v_{lm}|2l\hbar k_L\rangle$, where $v_{lm} = \langle v_{lm}|u_{q,\alpha}\rangle$ is coefficient of the Floquet state. τ is related to the modulation phase ϕ_1 and holding time t as $\tau = \frac{\omega_1 t + \phi_1}{2\pi} T$. It is also useful to define the overlapping between the Floquet state $|u_{q,\alpha}\rangle$ and a Bloch state $|n_q\rangle$ of the undriven potential as $P = \int_0^T |\sum_l \langle c_l(t)|n_q\rangle|^2 dt$. Property of the Floquet band is typically characterized by its most overlapping Bloch band [23]. Without loss of generality, our experiments are restricted to quasi-momentum $q = 0$, and energy gap between Bloch bands α and β are written as $\hbar\omega_{\alpha\beta}$. The technique can also be applied in systems with acceleration [12], which brings out phenomena different from our study.

When modulation phase ϕ_1 is given, a Floquet state can be projected into the momentum space, and such a state can be prepared by carrying out two lattice pulses with numerically designed pulse sequence [21, 22]. In the fast loading process, lattice depth of the two pulses is kept constant. For a target state, the fidelity of a prepared state can be given numerically for different pulse durations and time intervals, and the optimized pulse sequence is obtained by finding the maximum loading fidelity. Throughout this method we can get a loading fidelity of more than 95% experimentally.

With the initial modulation phase $\phi_1 = -\pi/2$, a pure Floquet state is loaded by lattice pulses

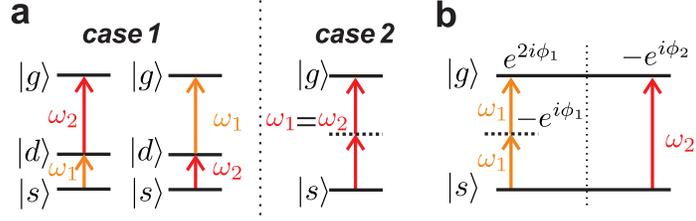


Fig. 4. (a) Two special cases in detecting the transfer population spectrum. In case 1, absorption of photons with ω_1 (orange) or ω_2 (red) is resonant with d band. In case 2, two frequencies are equal. (b) For s - g coupling ω_1 provides a two-photon process while $\omega_2 = 2\omega_1$ provides a one-photon process. Phases of two paths are controlled independently by modulation phases of ω_1 and ω_2 .

calculated with $\tau = \frac{\phi_1}{2\pi}T = -T/4$. For the same state, we also present a modulation with $\phi_1 = \pi/2$ to show the influence of modulation phase. The population on momentum components $|0\hbar k_L\rangle$ and $|\pm 2\hbar k_L\rangle$ for different initial phases $\phi_1 = -\pi/2$ and $\phi_1 = \pi/2$ are shown in Fig. 3(a1) and 3(a2) respectively. The parameters are $V_0 = 5.0E_r$, $V_1 = 0.5E_r$ and driven frequency is $\hbar\omega_1 = 5.0E_r$, red detuned from the band gap $\hbar\omega_{sd} = 5.2E_r$. Figure 3(a1) is a Floquet state, which shows a time period of $T = 2\pi/\omega_1 = 62.75\mu s$. The time evolution in momentum space would be quite different when the modulation phase is changing by π , as shown in Fig. 3(a2). Besides the oscillation with a frequency near ω_1 , we observe a slow growth of n_1 . Meanwhile, the amplitude of oscillations are also increasing following increase of the population on d band.

The influence of modulation phase is shown more clearly when taking time average in one modulation period T . In Fig. 3(b1) with $\phi_1 = -\pi/2$ the Floquet state shows a constant population in different momentum states by taking time average. While for $\phi_1 = \pi/2$, Fig. 3(b2) shows a Rabi oscillation between s - d bands with Rabi frequency E_F/\hbar , where E_F is the gap between two Floquet bands. The observation can also be explained by Eq. (5). The phase of coupling terms would change with ϕ_1 , thus the eigenstate is superposition of $|s\rangle$ and $|d\rangle$ with a relative phase determined by ϕ_1 . When the modulation phase is changed, the loaded state is no longer an eigenstate, and we can observe the Rabi oscillation.

5. Excitation of ground state via a double frequency modulation

The study of lattice modulation can be extended from single frequency to a more general form as described in Eq. (6). Specific to two-photon excitation between s - g band, the time dependent lattice is described as $V_L(t) = V_0 + V_1 \cos(\omega_1 t + \phi_1) + V_2 \cos(\omega_2 t + \phi_2)$, which includes seven parameters $V_0, V_1, V_2, \omega_1, \omega_2, \phi_1, \phi_2$. During the experiments, we mainly focus on the influence of modulation frequencies and phases, while keeping other parameters constant.

5.1. Spectrum of two-photon excitation

The single frequency modulation shows that ϕ_1 is related to relative phase between s and d band components of the Floquet state. However, with a nearly pure s band, the phase of single modulation can be neglected, only the phase difference between two modulations is important. Therefore, we chose $\phi_1 = \pi$ while leaving ϕ_2 variable to control the relative phase between two modulations.

For s - g band coupling through a two-photon absorption process, the sum of the two modulation frequencies is chosen as $\omega_1 + \omega_2 = \omega_{sg}$. This process is well described by Eq. (6), in

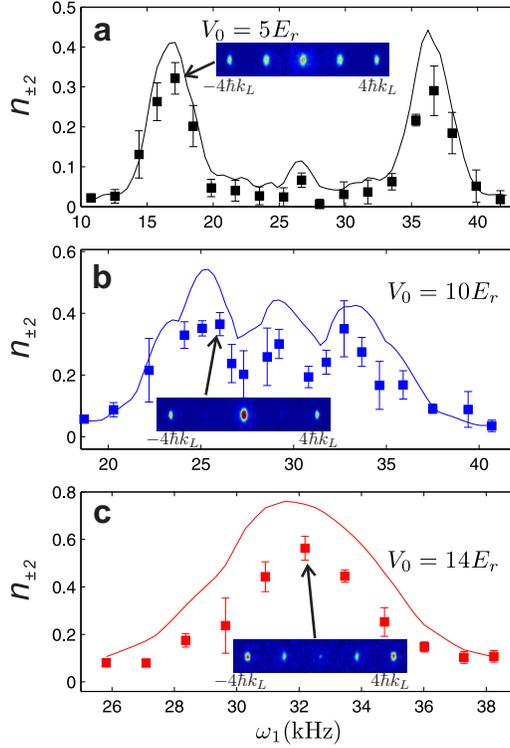


Fig. 5. Spectrum for the population on $\pm 4\hbar k_L$ states with increasing of modulation frequency ω_1 . Population detected on $\pm 4\hbar k_L$ after a double frequency modulation for (a) $V_0 = 5E_r$ (black) with $V_1 = 1.4E_r$, $V_2 = 1.6E_r$, $t = 300\mu s$, (b) $V_0 = 10E_r$ (blue) with $V_1 = 2.8E_r$, $V_2 = 2.2E_r$ and $t = 200\mu s$, (c) $V_0 = 14E_r$ (red) with $V_1 = V_2 = 2.5E_r$ and $t = 150\mu s$ are shown in rectangles with error bars. Solid lines are corresponding numerical simulation.

which we have considered different pumping paths, as schematically shown in Fig. 4(a). There are two cases which would benefit the excitation process.

Case 1: Resonant two-photon process. When $\omega_1 = \omega_{sd}$ or $\omega_2 = \omega_{sd}$, atoms are transferred from $|s\rangle$ to $|g\rangle$ with the assistance of d band as an intermediate band.

Case 2: Equal frequency two-photon process. When $\omega_1 = \omega_2 = \omega_{sg}/2$, two modulations with the same frequency can be added together, and the coupling strength of the process is doubled.

With resonance condition $\omega_1 = \omega_{sd}$ in **case 1**, when two modulation amplitudes are chosen as $V_1\Omega_{sd} = V_2\Omega_{dg}$ the transfer rate would show a maximum resonant peak. And we keep this modulation amplitudes while sweeping ω_1 . Modulation phase is chosen from numerical simulation to get a maximum transfer.

In the experiments, we sweep the frequency ω_1 for different lattice depths $V_0 = 5E_r$, $10E_r$ and $14E_r$. Population on momentum states $\pm 4\hbar k_L$ measured from the experiment are shown with rectangles in Fig. 5, comparing with the theoretical calculation shown in solid curves. Within the lattice depth we considered, g band is greatly concentrated on $|\pm 4\hbar k_L\rangle$ momentum states, thus $n_{\pm 2}$ can reflect transfer rate to g band.

Figure 5(a) shows the case of $V_0 = 5E_r$. For the lattice depth we have $\Omega_{sd}/\Omega_{dg} = 1.11$, correspondingly the modulation amplitudes are chosen as $V_1 = 1.4E_r$, $V_2 = 1.6E_r$, and $t = 300\mu s$. The holding time t may be chosen shorter if the maximum of numerical simulation is

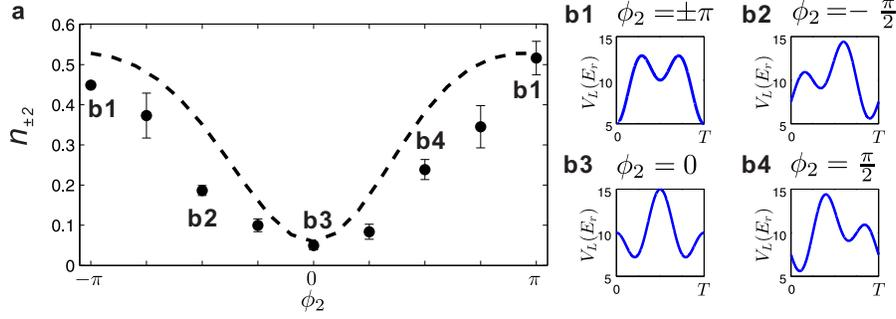


Fig. 6. The excited population on g band shows the interference between two paths. (a) Population transferred to $n_{\pm 2}$ is shown in black dots with error bars. The dashed line shows theoretical simulation for comparison. (b1)-(b4) V_L for different phases.

reached at an earlier time. In the figure, two peaks appear at $\omega_1 = \omega_{sd}$ and $\omega_2 = \omega_{sd}$ which follows **case 1** we have discussed. And there the central peak at frequency $\omega_1 = \omega_2$ following **case 2** is much lower than two peaks for **case 1**.

Figure 5(b) shows the spectrum with $V_0 = 10E_r$. With the increasing of V_0 , the energy difference ω_{sd} is getting closer to ω_{dg} , and three peaks are overlapping. Comparing with $V_0 = 5E_r$ the central peak is much higher, because the process of **case 2** is also near resonance with d band.

For $V_0 = 14E_r$ only one peak would be measured in the spectrum as shown in Fig. 5(c), which means **case 1** and **case 2** are fulfilled simultaneously. Under this condition, the coupling between s and g band is also greatly enhanced. Modulation amplitudes are $V_1 = V_2 = 2.5E_r$, for the two modulation frequencies are the same at **case 1** and can't be distinguished.

The experimentally detected peaks are governed by two cases, which are within the description of Eq. (6). Thus in the numerical simulation we can neglect higher order processes of emission and absorption of Floquet photons. The discrepancy between experimental result and the theoretical simulation is probably due to the influence of interaction and initial momentum distribution of the condensate. These effects would destroy coherency during the modulation, and the measured population of excited state would be lower than the maximum value in the theoretical simulation.

5.2. The role of modulation phases

When ω_1 and ω_2 are incommensurate, the influence of relative phase is not prominent because there is only one path for the pumping process and no states could interfere with each other. However, the effect of modulation phases would be more pronounced when two modulation frequencies are commensurate.

As shown in Fig. 4(b), when $2\omega_1 = \omega_2$, relative phase of modulations can be shown by performing a one-photon process simultaneously with a two-photon process. We choose the frequency $\omega_1 = \omega_{sg}/2$ at central peak of $V_0 = 10E_r$ lattice and the second modulation is performed with $\omega_2 = \omega_{sg}$. Modulation amplitudes are $V_1 = V_2 = 2.5E_r$ and $t = 500\mu s$. Similar to the process described by Eq. (6), in this problem we consider the interference between two states $|E_g - 2\hbar\omega_1\rangle$ and $|E_g - \hbar\omega_2\rangle$. During the two-photon process with $\phi_1 = \pi$, phase of state $|E_g - 2\hbar\omega_1\rangle$ remains zero, while ϕ_2 determine phase of state $|E_g - \hbar\omega_2\rangle$ as $\phi_2 - \pi$. Relative phase of two modulations is defined as $(\phi_2 - \pi) - \frac{\omega_2}{\omega_1}(\phi_1 - \pi) = \phi_2 - \pi$, and the interference can be changed from constructive to destructive with different ϕ_2 .

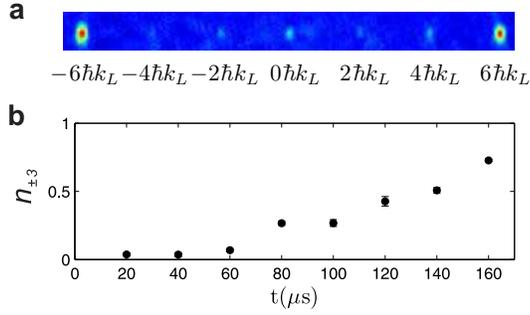


Fig. 7. A LMT beam splitter with a separation of $12\hbar k_L$. (a) TOF image of the LMT beam splitter. (b) Experimentally measured population of atom on momentum states $|\pm 6\hbar k_L\rangle$ are shown in black dots with error bars.

Figure 6(a) depicts the population transferred to g band with the phase of one-photon process changing by 2π . Figure 6(b) shows how the depth of lattice is varying with time for four different modulation phases. With $\phi_2 = \pi$, the population transferred to $|g\rangle$ through one-photon process and through two-photon process are in phase and the transfer rate is enhanced. When ϕ_2 is increasing, relative phase of two processes are deviating from zero, and the population on $|g\rangle$ would decrease. In the case of $\phi_2 = 0$ the two process are out of phase, and only few atoms can be transferred to g band. Further increasing of ϕ_2 would increase the measured population, and when ϕ_2 is changed by 2π the population on g band reaches the maximum value again.

The single atom Hamiltonian in Eq. (1) can well explain the excitation in our system. However, for the $500\mu\text{s}$ modulation, decoherence from mean-field interaction and the momentum distribution becomes significant, thus it is necessary to carry out a simulation based on the time-dependent Gross-Pitaevskii equation,

$$i\hbar \frac{\partial \Psi}{\partial t} = \left[-\frac{\hbar^2}{2m} \frac{\partial^2}{\partial x^2} + V_L(x, t) + \frac{1}{2} m \omega_x^2 x^2 + g |\Psi|^2 \right] \Psi, \quad (7)$$

where g is the parameter of interaction. In the simulation, we consider both the distribution of initial momentum and the mean-field interaction which would deduce the measured excitation rate. Dashed line in Fig.6(a) gives the result of simulation which fits well with the experiment. Similarly, the relative phase can also be changed by ϕ_1 of the two-photon process, which gives a period of π .

The collaborative effect of different frequency components is studied in two aspects, demonstrate the effect of both modulation frequencies and phases of different frequency components. The usefulness of this study is not limited to double frequency modulation, within these two aspects, collaborate effect of more frequency components can also be well understood.

6. Application in LMT beam splitter

The double frequency modulation can also be applied to realize a LMT beam splitter by pumping atoms to higher momentum states, which is useful in experiments of atomic interferometry [24]. According to the resonant condition we have discussed, a preferred choice is $V_0 = 14E_r$ with the modulation frequency $\omega_1 = \omega_{sd} = \omega_{dg}$. The other modulation frequency is chosen as $\omega_2 = \omega_{gi}$ (with i the 6^{th} excited Bloch band) to get a distribution at $\pm 6\hbar k_L$.

We begin with a condensate, the lattice is suddenly turn on, modulated with $V_1 = V_2 = 2.5E_r$ and the preferable phases are found numerically. A TOF image of experimental result is shown in Fig. 7(a). Figure 7(b) shows the population of atoms on momentum states $|\pm 6\hbar k_L\rangle$ where we

have subtracted the thermal gas. Near 80% of the atoms are coherently transferred into $\pm 6\hbar k_L$ momentum states within $160\mu s$, and the maximum lattice depth needed is below $V_0 + V_1 + V_2 = 24E_r$. Comparing with a LMT beam splitter based on high order Bragg scattering [16], our method needs a much lower lattice depth and is easy in practice. Furthermore, the process is symmetric for both sides, and would not introduce phase shift between two separated atom clouds.

A momentum splitting of $12\hbar k_L$ is not the limit of the amplitude modulation. More frequency components or another subsequent modulation can be introduced to reach a larger momentum splitting. For example, after the double frequency modulation, by performing another single frequency modulation resonance with the energy difference between $|\pm 6\hbar k_L\rangle$ and $|\pm 8\hbar k_L\rangle$ momentum states, the atoms can be transferred to $|\pm 8\hbar k_L\rangle$ coherently.

7. Discussion and conclusion

Following Floquet-Bloch theory we have presented an experimental preparation of a Floquet state and study its property. The non-adiabatic loading method would take much less time and greatly reduce the heating problem. The loading method could also be extended to systems with a shaken lattice [7] or a combined modulation [6, 23], which provides a several millisecond longer lifetime for condensate in the experimental study on areas including the detection of Floquet topological states [17, 25, 26].

In conclusion, based on the study of single frequency modulation, we investigate double frequency modulation in detail. Experimental observations show that different modulation frequency components would influence each other in two ways. When two frequencies are resonant with subsequent excitation processes, the modulation can induce a resonant two photon process which can effectively transfer atoms to higher excited bands. With specific modulation frequencies, interference between a one-photon path and a two-photon path is observed, revealing influence of modulation phases when two frequencies are commensurate. The quantum interference can be used to enhance the excitation rate or destruct unwanted excitations. Using the technique of double frequency modulation, we also demonstrate an efficient way to realize a LMT beam splitter with low lattice depth. Our study provides a more flexible way to coherently control quantum states through an optical lattice.

Acknowledgments

This work is partially supported by the state Key Development Program for Basic Research of China No.2011CB921501, NSFC (Grants No.61475007, No.11334001 and No.91336103), RFDP (Grants No.20120001110091).